Journal of Applied and Natural Science
16(2), 865 - 873 (2024)
ISSN : 0974-9411 (Print), 2231-5209 (Online)
journals.ansfoundation.org

Research Article

Targeting NSP-13 protein of SARS CoV-2 with selected natural compounds: An *in-silico* approach

Divya Sharma
Department of Bio and Nano Technology, Guru Jambeshwar University of Science and Technology (GJUS &T), Hisar (Haryana), India
Anita Rani Gill
Department of Bio and Nano Technology, Guru Jambeshwar University of Science and Technology (GJUS &T), Hisar (Haryana), India
Poonam Bansal
Department of Biosciences and Technology, Maharishi Markandeshwar (Deemed to be) University, Mullana (Haryana), India
Soniya Goyal
Department of Biosciences and Technology, Maharishi Markandeshwar (Deemed to be) University, Mullana (Haryana), India
Pooja Sharma*
Department of Biosciences and Technology, Maharishi Markandeshwar (Deemed to be) University, Mullana (Haryana), India
Moyad Shahwan
Centre of Medical and Bio-Allied Health Sciences Research, Ajman University, Ajman 346, United Arab Emirates;
Department of Clinical Sciences, College of Pharmacy and Health Sciences, Ajman University, Ajman 346, United Arab Emirates
Seema Ramniwas
University Centre for Research & Development, University Institute of Pharmaceutical Sciences, Chandigarh University, Gharuan, Mohali (Punjab), India
Hardeep Singh Tuli*
Department of Biosciences and Technology, Maharishi Markandeshwar (Deemed to be) University, Mullana (Haryana), India

*Corresponding author : E-mail: pooja0029@gmail.com

Article Info
https://doi.org/10.31018/jans.v16i2.5647
Received: April 06, 2024
Revised: June 05, 2024
Accepted: June 09, 2024

How to Cite
Sharma, D. *et al*. (2024) Targeting NSP-13 protein of SARS CoV-2 with selected natural compounds: An *in-silico* approach. *Journal of Applied and Natural Science*, 16(2), 865 - 873. https://doi.org/10.31018/jans.v16i2.5647

Abstract
SARS-CoV-2 swiftly spread in Wuhan, China, leading to a pandemic crisis worldwide. Genome sequence analysis of this virus revealed a close analogy with its closely related strains, SARS-COV and MERS-COV. In the case of SARS-CoV-2, Nonstructural protein 13 (NSP13), also known as helicase, has been identified as a target for reducing the severity of infection due to its high sequence conservation and essential role in viral replication. NSP13 helicase structure in SARS-CoV-2 differs only by one amino acid from the SARS-CoV helicase structure. Targeting NSP13 with natural compounds holds significant potential for developing safe and effective antiviral therapies utilizing advanced computational approaches. The properties of 8 different natural compounds, i.e. Imidazole, Pyrrole, Tropolone, Benzotriazole, Imidazodiazepine, Phenothiazine, Acridone and Bananin were screened by applying Lipinski's rule of five, ADME (absorption, distribution, metabolism, and excretion) properties, and Radar plots to discover their drug efficacy at a target site, safety, and absorption. Docking studies confirmed Bananin with a binding affinity of -7 kcal/mol as a potential inhibitor of NSP13 of SARS-CoV-2 with better pharmacokinetics, drug likeliness, and oral bioavailability. Based on the *in silico* study, it is suggested that Bananin shows promising effects against NSP13 protein, forming a maximum number of hydrogen bonds exhibiting higher binding affinity. This stronger affinity indicates a stronger interaction between the compound and its target, potentially leading to enhanced biological activity and therapeutic efficacy. This novel study has unlocked the door for a prospective SARS-CoV-2 inhibition strategy and developing antiviral interventions targeting NSP13 based on molecular docking.

Keywords: Antiviral therapies, Molecular Docking, Natural Compounds, Nonstructural proteins, SARS COV-2

INTRODUCTION

The immensely contagious viral COVID-19 caused by severe acute respiratory coronavirus 2 (SARS COV-2) is the most deleterious pandemic in 21st century, emerging as the most consequential global health crisis. *Corona viridae* is a large family which includes various genera such as Alpha coronavirus, Beta coronavirus, Gamma coronavirus, and Delta coronavirus (Fan *et al.*, 2019). Human Coronaviruses (HCOVs) include 7 strains *HCov-229E, HCov-OC43, HCoV NL63, HCoV-HKU1, SARS-CoV* (severe acute respiratory syndrome coronavirus), and MERS-CoV (middle east respiratory syndrome coronavirus) that cause illness ranging from the common cold to more severe diseases (Andersen *et al.*, 2020) It was reported that the spread of this virus leads to mutations that give rise to new variants, more deadly than the original infection. Severe Acute Respiratory Syndrome Coronavirus-2 (SARS-COV-2) emerged in November 2019 and belongs to Beta coronaviruses. The SARS-COV2 (B.1.617) lineages include three main subtypes B.1.617.1, B.1.617.2, and B.1.617.3. In India B.1.617.2 lineage variant started affecting the population by late 2020 with a 60% more transmissible than the Alpha variant (B.1.1.7). Intense cases due to this variant has distressed the condition and has been added to the list of variants of concern (VOCs) (Baral *et al.*, 2021; Pal *et al.*, 2020). SARS-CoV2 is a non-segmented double-layered lipid-enveloped virus (Rastogi *et al.*, 2020), (Naqvi *et al.*, 2020) with 50–200 nm in diameter(N. Chen *et al.*, 2020). It has a linear RNA genome of 29.9 kb in size (Rastogi *et al.*, 2020), which contains 38 % GC content. However, the genome comprises U (32.2%), followed by A (29.9%), and G (19.6 %), and C (18.3 %) (Astuti and Ysrafil, 2020). The whole genome of SARS-CoV2 encodes approximately 7096 residues long polyproteins, which consist of many structural and nonstructural proteins (NSPs). The structural protein comprises the outer structure of the virus whereas nonstructural proteins help in viral replication and viral assembly (Rastogi *et al.*, 2020). Furthermore, SARS CoV2 is made up of 14 ORFs (open reading frames) arranged from 5' to 3', also known as the 5' and 3' UTRs (untranslated regions) (Rastogi *et al.*, 2020). The first ORF comprises 67% of the genome that encodes nonstructural proteins (NSPs) and the remaining ORF codes for structural and accessory proteins. Sequence variation among SARS-CoV-2 and SARS-CoV revealed no significant difference in ORFs and NSPs. In a nutshell, 5’ UTR replicase complex (ORF1a and ORF1b) encodes for nonstructural proteins while 3’ UTR region encodes for structural proteins like spike proteins (S), nucleocapsid proteins (N), envelope protein (E) and membrane glycoprotein (M). The present review carried out computational docking of NSP13 (SARS CoV-2) against natural compounds.

Detailed structure and function of *NSP13*

The nonstructural protein 13 (NSP13), a 67 kDa, belongs to the 1B superfamily of helicases (Tanner *et al.*, 2003). It uses the hydrolysis energy of NTPs to catalyse the unwinding of double-stranded DNA or RNA in the 5' to 3' direction (Tanner *et al.*, 2003). NSP13 comprises of 5 domains, an N-terminal zinc-binding domain (ZBD) that coordinates 3 structural zinc ions, a coiled "stem" domain, a beta-barrel 1B domain, and two "RecA-like" helicase subdomains (1A and 2A), which are responsible for the binding and hydrolysis of nucleotides (Newman *et al.*, 2021), (J. Chen *et al.*, 2020). The N-terminus of NSP13 contains 26 cysteine residues, 14 of which are highly conserved and predicted to form a Zn2+ nuclear binding cluster important for helicase activity *in vitro*. In addition, some of these cysteine residues may participate in disulphide bridges, and these appear to increase helicase activity (Subissi *et al.*, 2014). It has been observed that NSP13 interacts with the viral RNA-dependent RNA polymerase NSP12 and acts synergistically with the NSP7/NSP8/NSP12; replication transcription complex. Through mechanistic regulation, this interaction potentially stimulates the NSP13 helicase property. In addition to helicase activity, NSP13 possesses 5’RNA triphosphatase activity in the same active site, suggesting an even more essential role for NSP13 in the formation of the viral 5' mRNA cap (Neuman *et al.*, 2006). A helicase protein binds NTP using two structurally common amino acid sequences named motif I (Walker A/Boxes A) and motif II (Walker B/Boxes B) (Walker *et al.*, 1982). Motif I is a phosphate-binding P-loop that interacts with the ribose sugar while motif II is a Mg^{2+} cofactor.

Comparative analysis among closely related strains

The genomic arrangement of ORFs is quite similar to that of SARS-CoV and MERS-CoV. Their proteins have high degree of sequence similarity to the equivalent proteins of SARS-CoV and MERS-CoV (Smith *et al.*, 2013), (Lu *et al.*, 2020). The virus had a 79.0% sequence identity with SARS-CoV and an even greater sequence identity of about 86.7% -89% with MERS-CoV (Chan *et al.*, 2020). The majority of these SARS-CoV-2 nonstructural proteins have more than 85% amino acid sequence identity with SARS-CoV. The comparative analysis between SARS-COV, SARS-COV2, and MERS-COV considering NSP13 protein has been inserted in Table 1.

Certain drugs such as azithromycin, nitazoxanide, and cefoperazone (Mostafa *et al.*, 2020) (Eweas *et al.*, 2022) have been reported against SARS-COV2 spike proteins in literature, but targeting the core nonstructural proteins is still a hindrance as multiple potential drugs are currently in clinical trials for the treatment.

Table 1. Comparative analysis of SARS-COV, MERS-COV and SARS-COV2

Species	Features						
	Name	**Function**	**Domain Structure**	**Sequence Similarity**	**Evolutionary Origin**	**Mutation Rate**	**Clinical Relevance**
SARS- COV	Non-Structural Protein 13 (NSP-13)	Helicase-Facilitate Viral replication	Conserved Helicase Domains	Highly Similar (98%)	Beta Coronavirus	Low	SARS Outbreak 2002-2003
MERS-COV				Less Similar (60-70%)			MERS Outbreak 2012
SARS-COV 2				Highly Similar (98%)			Covid pandemic since 2019

Several mutations in structural proteins that act against therapeutic drugs lead to new coronavirus variants. It has been found that some of the natural compounds are much more potent against viral infection, so they may work against COVID-19's upcoming variants. Imidazole is a nitrogen-containing hetero-cyclic class of amphoteric compounds. It is an antifungal and antiviral drug that already acts against many life-threatening viruses like zika, dengue, hepatitis, HIV and influenza viruses (Andersen *et al.*, 2020). Pyrrole is another biologically active derivative that serves as antimicrobial, anti-cancerous, anti-inflammatory, antiviral and enzyme -inhibiting drug (Gholap, 2016). This drug is approved for human therapeutic use against the vaccinia virus as it inhibits protein synthesis and DNA binding (Khramtsova *et al.*, 2021). Similarly, Tropolone is a pharmacological derivative and antibacterial, antiviral, antifungal antitumor, anti-inflammatory, antioxidant, and insecticidal properties. It also works against NSP3 (Helicase) protein of Hepatitis C virus (Borowski *et al.*, 2007). Benzotriazole mimics the natural purine and pyrimidine chemical structures, intervening as false substrates for performing biological function and resulting as antibacterial or antiviral agents (Ibba *et al.*, 2021). Bananin is an adamantane-related antiviral drug that acts against SARS-COV's helicase, further inhibiting viral replication. The present study applied the same approach against SARS-COV2 to evaluate the effect of natural compounds. *In-silico* studies reveal that one of the above-mentioned drugs, Bananin, negatively affects the DNA complex stability, resulting in altered replication activity, which opens a new bridge for advancing several anti-SARS COV agents that provide a promising novel strategy to inhibit the COV2 replication.

MATERIALS AND METHODS

Retrieval of receptor three-dimensional structure

The three-dimensional crystal structure of the NSP 13 Protein with PDB ID: 6ZSL with a resolution of 1.94 Å was downloaded from the online database Research Collaboratory Structural Bioinformatics-Protein Data Bank; RCSB-PDB (www.rcsb.org) . The protein model was prepared for docking by deleting water molecules and heteroatoms (Fig. 1)

Ligand's preparation and analysis of ADME properties

For virtual screening, eight ligands were selected. The 3-D structure of these ligands was retrieved from the PubChem database in SDF format. The Ligand library was created to determine their ADME (absorption, distribution, metabolism, and excretion) properties. (Jayaram *et al.*, 2012). SWISS ADME software was employed to evaluate Lipinski's rule of five. In this rule, physiochemical properties such as molecular weight (<500 KDa), H-bond donor (5), H bond acceptor (<10), Log P (<5), and drug likeliness were considered for the profiling of all the ligands (Lipinski, 2004).

Molecular docking of ligands with NSP13 protein

PyRx v0.8 software is utilized for virtual screening and binding energy studies. First, energy minimization is applied for ligands using a Universal Force field (UFF). The target protein was converted into a macromolecule. Open Bable feature in PyRx converts the chosen ligands into PDBQT format (O'Boyle *et al.*, 2011). Docked structure of a macromolecule and ligand with the highest binding affinity were interpreted using Discovery studio visualizer and PYMOL.

Rule of five (RO5)

Lipinski's RO5 (Rule of Five) analysis is used for evaluating the drug-likeness of a compound, a mandatory step in determining if a specific compound could probably be orally active. ligands were analyzed for RO5 using a Supercomputing facility for bioinformatics and computational biology (http://www.scfbio-iitd.res.in/software/drugdesign/lipinski.jsp) in this method (Jayaram *et al.*, 2012; Lipinski, 2004).

In Silico ADME (Adsorption, Distribution, Metabolism, and Excretion) analysis

Various pharmacokinetic characteristics, including Absorption, Distribution, Metabolism, and Excretion, were assayed through Swiss ADME software (http://www.swissadme.ch/index.php). This analysis aims to generate information that will assist in developing new drugs.

Bioavailability radar

The bioavailability radar ligands were calculated through Swiss ADME (http://www.swissadme.ch/index.php), which immediately determines whether a compound is orally bioavailable or not.

RESULTS AND DISCUSSION

Natural compounds play an essential role in viral infections, including influenza, MERS, SARS-COV (Abdelrahman *et al.*, 2020). The present study chose eight ligands against SARS-COV, and out of these, Bananin showed remarkable potential against the targeted molecule. Various Covid variants may even show promising effectiveness against Bananin targeting the same receptor (Perez-Lemus *et al.*, 2022; Wang *et al.*, 2011). Based on the docking studies, it was suggested that these phytochemicals are potent molecules to be tested against SARS-CoV-2 and can be used to develop effective antiviral drugs.

A computational approach is applied to discover a potential drug for the stand-up treatment against this particular virus. *In silico* virtual docking depends on ligand binding with the target molecule where its active site is tested against the ligand, and the binding score is calculated. A ligand with the highest binding affinity and lowest binding energy is further considered a potential one. The binding affinity of chosen ligands has been scored out. Tropolone, Acridone, Bananin, Imidazodiazepine, Phenothiazine, Benzotriazole, Imidazole, Pyrrole have binding affinity in the range of -2.5 to -7.5 Kcal/mol with receptor molecules as shown in Table 4. Docking studies revealed that Bananin showed a significant binding affinity of -7.3 kcal/mol, preferably the highest among the studied eight ligands. It interacts with Asn179, His554, Asp534, Arg560, Thr410, Arg 409, and Ala 407 residues of NSP13 protein of SARS COV-2 through covalent hydrogen bonding while Pro406, Leu405, Leu412, Pro408, Leu417 residues formed van der Waal force of interaction with ligand. The docked pose of receptors and ligands is presented in Fig. 1.

In silico results predicted that natural compounds interrupt the attachment of RNA polymerase to NSP13 and no further unwinding of double-stranded RNA has been shown; hence RNA polymerase action terminates. It is reported that Bananin acts as a potent effector drug against SARS-COV (Tanner *et al.*, 2005). Similarly, docking results confirm that Bananin can be used as anti-COVID agent due to a significant binding affinity of -7.3 kcal/mol.

Pharmacokinetic and drug likeness screening of drugs

The properties of 8 selected drugs were screened using Lipinski's rule of five and *in silico* ADME analysis followed by the determination of bioavailability radar and bioavailability scores of ligands. The five parameters of all selected drugs, such as molecular weight, hydrogen donor, hydrogen acceptor, lipophilicity and molar refractivity, were checked using Lipinski's rule (Jayaram *et al.*, 2012; Lipinski, 2004). The selected drugs, such as Imidazole, Pyrrole, Tropolone Benzotriazole, Imidazodiazepine, Phenothiazine, Acridone and Bananin satisfied all five criteria of Lipinski's rule as presented in Table 2 and further screened for ADME analysis using SwissADME tool (freely available web tool used for prediction and evaluation of pharmacokinetics and drug-likeness of molecules built on several models) (Daina *et al.*, 2017). *In silico* pharmacokinetics and drug-likeness of selected ligands are shown in Table 3.

The estimated solubility (ESOL) showed that the drug Bananin is more soluble among all selected molecules. Lipophilicity written as iLOGP affects the absorption of the drug; the lower the iLOGP value, greater will be the absorption of the drug, and *vice versa*. Based on lipophilicity and polarity of compounds, the gastrointestinal absorption (GIA) and blood-brain barrier (BBB) permeation are anticipated through a BOILED model (Daina and Zoete, 2016). All selected compounds showed high gastrointestinal absorption (GIA) and the bioavailability score of all selected ligands falls in the normal range, i.e. 0.55. All ligands except Phenothiazine are non-substrate of p-glycoproteins most preferable for oral bioavailability. Drugs that are substrates to p-glycoprotein have the potential to reduce permeability, absorption, retention time of drugs, and oral bioavailability(Amin, 2013; Lin and Yamazaki, 2003). As shown in Table 2, most of the ligands are non-inhibitors of CYP3A4 and CYP1A2 (members of drug-metabolizing enzymes cytochrome P450, which possesses a vital role in drug metabolism). If a drug is a substrate of any CYP isoenzyme, it could result in rapid metabolism causing undesirable accumulation of the drug (Ji *et al.*, 2020). Therefore, *in silico* analysis plays a vital role in drug development by predicting ligands' interaction with cytochrome P450 isoenzymes.

Bioavailability radar

The graphical representation of bioavailability radar gives a rapid assessment of the drug-likeliness of a molecule. As shown in Fig. 2, the pink area indicates the optimal range of each parameter, including lipophilicity, molecular weight, polarity, flexibility, and solubility. A drug is said to be orally bioavailable when it is not too lipophilic, has small molecules, is polar, and is not too flexible. The prediction of whether ligands are orally bioavailable can only be confirmed if the compound falls under the pink area of the radar plot. Among all parameters, flexibility and polarity are two mandatory parameters in the prediction of the bioavailability of compounds. Flexibility (FLEX) is determined by number of rotatable bonds, which should be not

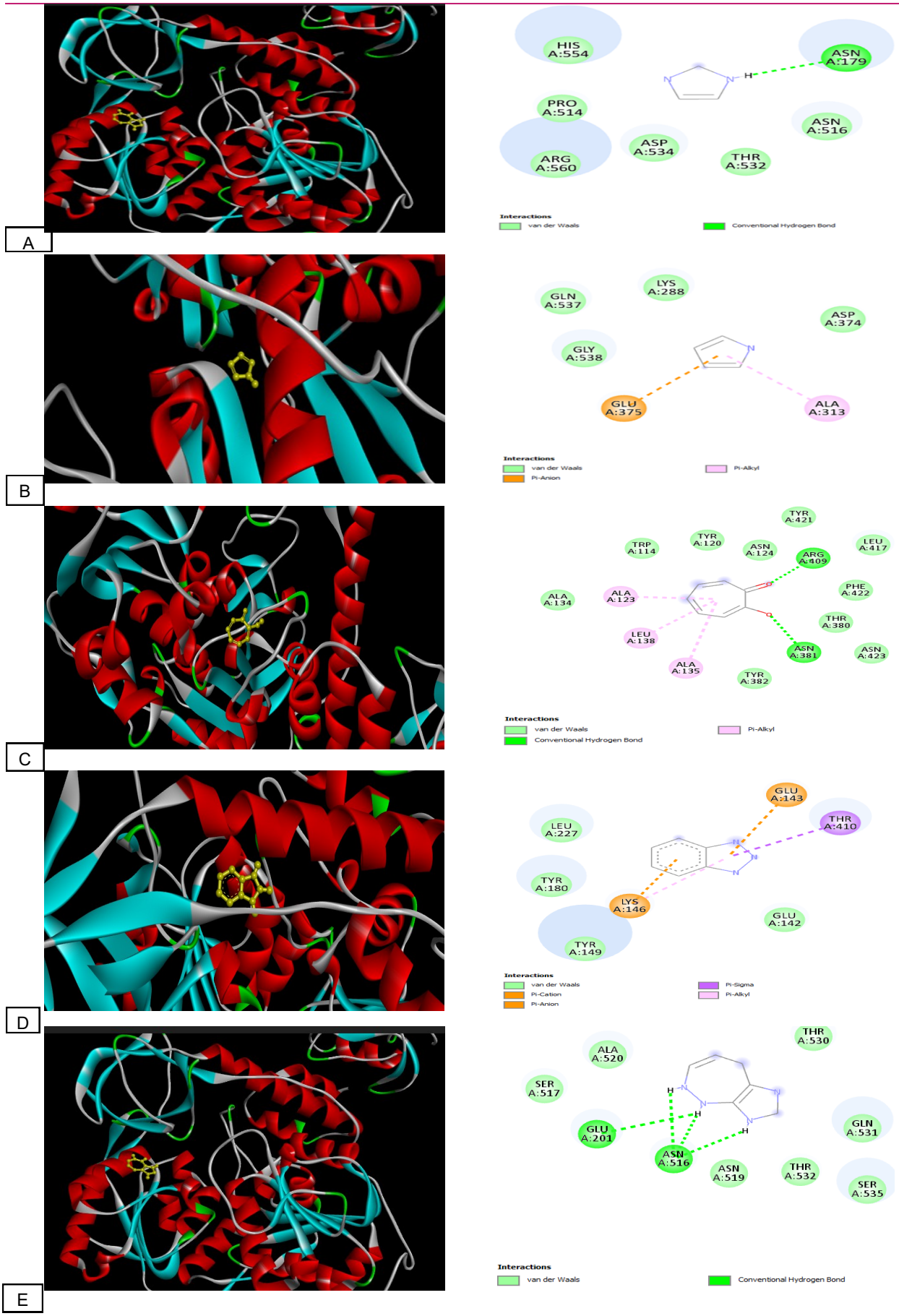
A
HIS A:554
ASN A:179
PRO A:514
ASN A:516
ASP A:534
ARG A:560
THR A:532
Interactions
van der Waals
Conventional Hydrogen Bond
B
GLN A:537
LYS A:288
ASP A:374
GLY A:538
GLU A:375
ALA A:313
Interactions
van der Waals
Pi-Anion
Pi-Alkyl
C
TYR A:421
TRP A:114
TYR A:120
ASN A:124
LEU A:417
ARG A:409
ALA A:134
ALA A:123
PHE A:422
THR A:380
LEU A:138
ASN A:381
ASN A:423
ALA A:135
TYR A:382
Interactions
van der Waals
Conventional Hydrogen Bond
Pi-Alkyl
D
GLU A:143
LEU A:227
THR A:410
TYR A:180
LYS A:146
GLU A:142
TYR A:149
Interactions
van der Waals
Pi-Cation
Pi-Anion
Pi-Sigma
Pi-Alkyl
E
THR A:530
ALA A:520
SER A:517
GLU A:201
GLN A:531
ASN A:516
ASN A:519
THR A:532
SER A:535
Interactions
van der Waals
Conventional Hydrogen Bond

Fig. 1. *Contd…….*

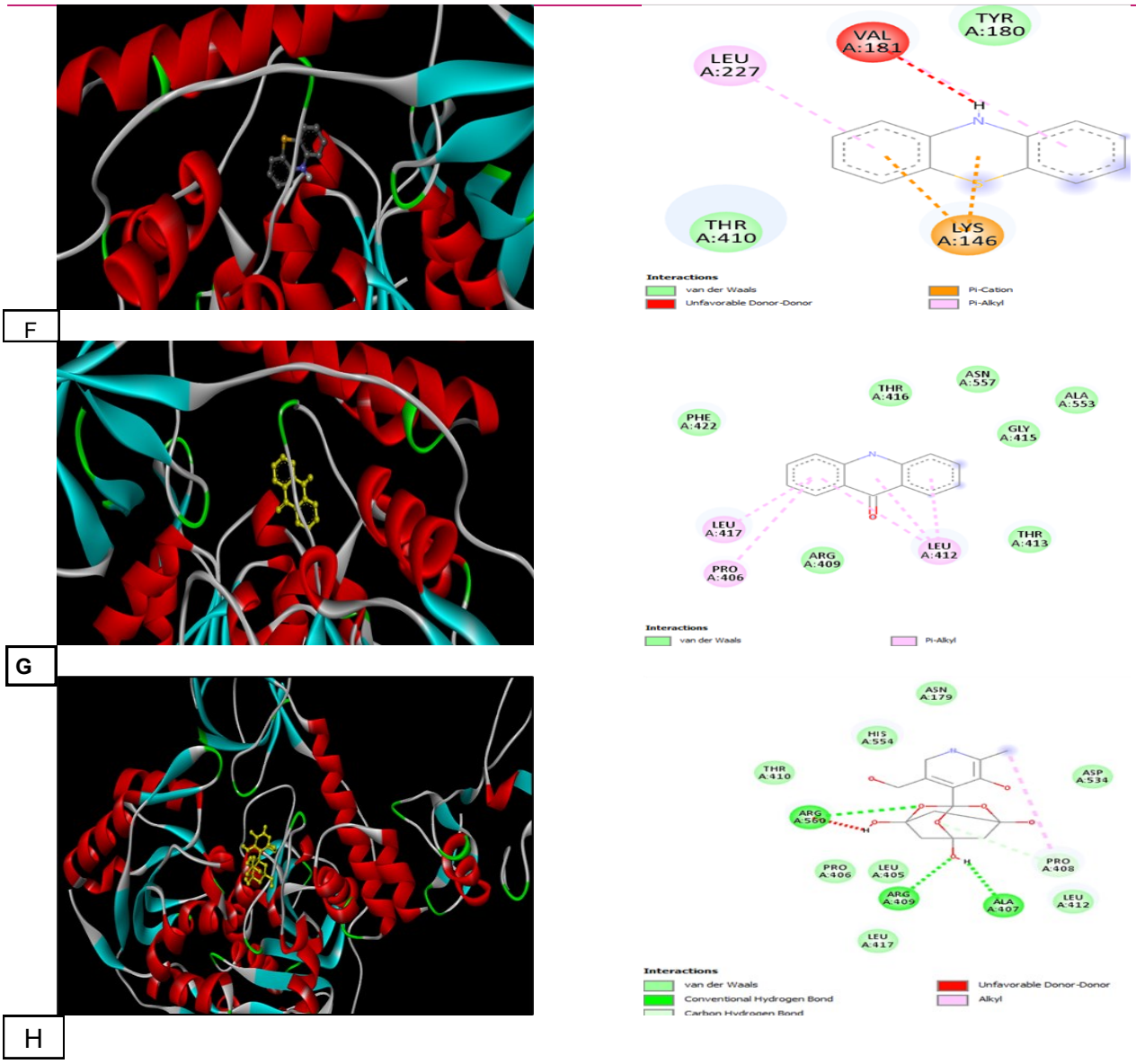

Fig. 1. *Showing 3-D and 2-D interactions of NSP13 protein with studied ligands; Imidazole (A) Pyrrole (B) Tropolone (C) Benzotriazole (D) Imidazodiazepine (E) Phenothiazine (F) Acridone (G) Bananin (H)*

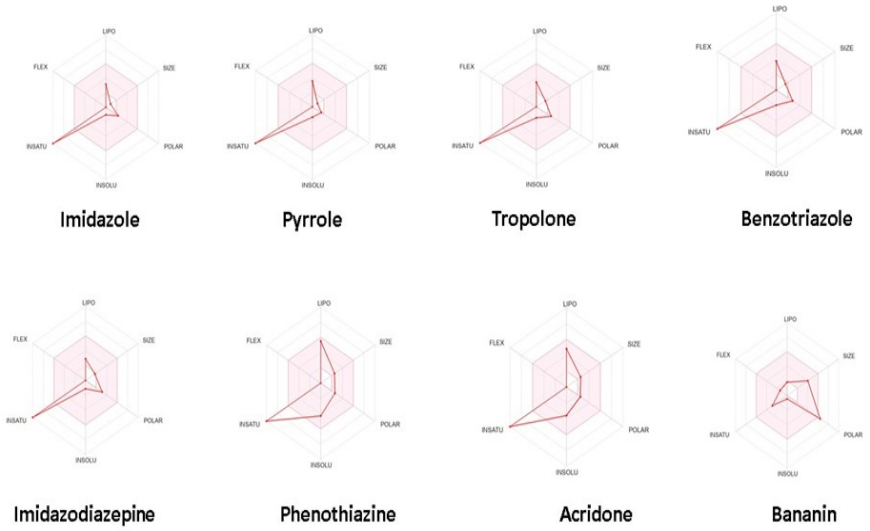

Fig. 2. *Showing radar plots of ligands' characteristics including lipophilicity, molecular weight, polarity, insolubility, in saturation and flexibility* (pink area indicatings the optimal range of each parameter)

Table 2. Lipinski rule of five

S.No.	Ligands	Mass	Hydrogen Donor	Hydrogen Acceptor	LogP	Molar refractivity
1	Imidazole	68.0	1	1	0.40	18.58
2	Pyrrole	67.0	1	0	1.01	20.79
3	Tropolone	122.0	1	2	1.12	33.98
4	Benzotriazole	119.0	1	2	0.95	33.88
5	Imidazodiazepine	132.0	0	4	0.07	35.06
6	Phenothiazine	199.0	1	0	3.94	62.45
7	Acridone	195.0	1	2	2.97	59.59
8	Bananin	327.0	5	9	0.50	70.19

Table 3. Pharmacokinetics study of LogS, ESOL, BBB, P-gp substrate, CYP1A2 inhibit, CYP3A4 inhibitor, iLOGP, Bioavailability Score

S. No.	Ligands	ESOL (LogS)	GIA	BBB Permeant	P-gp sub-strate	CYP1 A2 inhibit or	CYP3 A4 Inhibit or	(iLOGP)	Bioavail-ability Score
1	Imidazole	-1.51	High	Yes	No	No	No	1.41	0.55
2	Pyrrole	-1.41	High	Yes	No	No	No	0.01	0.55
3	Tropolone	-1.51	High	Yes	No	No	No	1.41	0.55
4	Benzotriazole	-1.96	High	Yes	No	No	No	0.59	0.55
5	Imidazodiazepine	-1.15	High	No	No	No	No	0.84	0.55
6	Phenothiazine	-4.32	High	Yes	Yes	Yes	Yes	2.21	0.55
7	Acridone	-3.62	High	Yes	No	Yes	Yes	1.94	0.55
8	Bananin	-0.48	Low	No	No	No	No	1.40	0.55

LogS refers to ligands considering certain parameters; **ESOL** refers to the calculation of the water solubility of a drug compound; **GIA**: refers to the rate of gastrointestinal absorption of a drug molecule; **BBB permeability** refers to the ability of ligands to cross the blood-brain barrier and reach their target within the brain to exert a therapeutic effect; **P-gp substrate**: indicates ligand transported by P-gp membrane protein to efflux from the cells; **CYP1A2 and CYP3A4 inhibitor** (Cytochrome P450) properties represent whether ligands allow to inhibit the activity of these inhibitors that are responsible for affecting the metabolism of substrates; **ILOGP** refers to the lipophilicity of ligand molecules; **Bioavailability score** measures the fraction of drugs/ligands that reach the systematic circulation in the body after administration, compared to a dose administered intravenously. It is expressed in percentage.

Table 4. Binding affinity of ligands

S.No.	Ligand Molecules	Binding Affinity (kcal/mol)
1	Imidazole	-2.9
2	Pyrrole	-3.2
3	Tropolone	-5.3
4	Benzotriazole	-5.3
5	Imidazodiazepine	-5.5
6	Phenothiazine	-6.0
7	Acridone	-6.4
8	Bananin	-7.0

more than 9 bonds, and polarity (POLAR) is shown by TPSA (topological polar surface) not more than 20 $A^0$2 (Ji *et al.*, 2020). Among all selected drugs, only Bananin was noted to satisfy radar plot criteria and hence can be of choice to be orally bioavailable, as illustrated in Fig. 2.

Conclusion

The progress and development of vaccines/drugs have quickly reached the epitome of the fight against the deadly virus. Natural compounds, including influenza, MERS, SARS-COV and SARS-COV-2, are essential for viral infection therapies. Targeting the NSP13 (helicase) of SARS-COV-2 by using non-competitive inhibitors may show a promising way to play the role of antiviral target. In the present study, among eight ligands (Tropolone, Acridone, Pyrrole, Imidazodiazepine, Phenothiazine, Benzotriazole, Imidazole, and Bananin) selected against NSP13 of SARS-COV as a target molecule, only one ligand Bananin showed the highest binding affinity against the target molecule and can be used as an anti-SARS CoV agent. These innovative approaches can be a turning point in combating the COVID-19 pandemic and may potentially provide more target information for drug design.

Conflict of interest

The authors declare that they have no conflicts of interest.

REFERENCES

1. Abdelrahman, Z., Li, M. & Wang, X. (2020). Comparative review of SARS-CoV-2, SARS-CoV, MERS-CoV, and Influenza A Respiratory Viruses. *Frontiers in Immunology*, 11. https://doi.org/10.3389/fimmu.2020.552909

2. Amin, Md. L. (2013). P-glycoprotein Inhibition for Optimal Drug Delivery. *Drug Target Insights*, 7, DTI.S12519. https://doi.org/10.4137/DTI.S12519
3. Andersen, K. G., Rambaut, A., Lipkin, W. I., Holmes, E. C. & Garry, R. F. (2020). The proximal origin of SARS-CoV-2. In *Nature Medicine*, 26 (4), 450–452. Nature Research. https://doi.org/10.1038/s41591-020-0820-9
4. Astuti, I. & Ysrafil. (2020). Severe Acute Respiratory Syndrome Coronavirus 2 (SARS-CoV-2): An overview of viral structure and host response. *Diabetes and Metabolic Syndrome: Clinical Research and Reviews*, 14 (4), 407–412. https://doi.org/10.1016/j.dsx.2020.04.020
5. Baral, P., Bhattarai, N., Hossen, M. L., Stebliankin, V., Gerstman, B. S., Narasimhan, G. & Chapagain, P. P. (2021). Mutation-induced changes in the receptor-binding interface of the SARS-CoV-2 Delta variant B.1.617.2 and implications for immune evasion. *Biochemical and Biophysical Research Communications*, 574, 14–19. https://doi.org/10.1016/j.bbrc.2021.08.036
6. Borowski, P., Lang, M., Haag, A. & Baier, A. (2007). Tropolone and its derivatives as inhibitors of the helicase activity of hepatitis C virus nucleotide triphosphatase/helicase. *Antiviral Chemistry & Chemotherapy*, 18 (2), 103–109. https://doi.org/10.1177/095632020701800206
7. Chan, J. F. W., Kok, K. H., Zhu, Z., Chu, H., To, K. K. W., Yuan, S. & Yuen, K. Y. (2020). Genomic characterization of the 2019 novel human-pathogenic coronavirus isolated from a patient with atypical pneumonia after visiting Wuhan. *Emerging Microbes and Infections*, 9 (1), 221–236. https://doi.org/10.1080/22221751.2020.1719902
8. Chen, J., Malone, B., Llewellyn, E., Grasso, M., Shelton, P. M. M., Olinares, P. D. B., Maruthi, K., Eng, E. T., Vatandaslar, H., Chait, B. T., Kapoor, T. M., Darst, S. A. & Campbell, E. A. (2020). Structural Basis for Helicase-Polymerase Coupling in the SARS-CoV-2 Replication-Transcription Complex. *Cell*, 182 (6), 1560-1573.e13. https://doi.org/10.1016/j.cell.2020.07.033
9. Chen, N., Zhou, M., Dong, X., Qu, J., Gong, F., Han, Y., Qiu, Y., Wang, J., Liu, Y., Wei, Y., Xia, J., Yu, T., Zhang, X., & Zhang, L. (2020). Epidemiological and clinical characteristics of 99 cases of 2019 novel coronavirus pneumonia in Wuhan, China: a descriptive study. *The Lancet*, 395 (10223), 507–513. https://doi.org/10.1016/S0140-6736(20)30211-7
10. Daina, A., Michielin, O. & Zoete, V. (2017). SwissADME: a free web tool to evaluate pharmacokinetics, drug-likeness and medicinal chemistry friendliness of small molecules. *Scientific Reports*, 7, 42717. https://doi.org/10.1038/srep42717
11. Daina, A., & Zoete, V. (2016). A BOILED□Egg To Predict Gastrointestinal Absorption and Brain Penetration of Small Molecules. *ChemMedChem*, 11 (11), 1117–1121. https://doi.org/10.1002/cmdc.201600182
12. Eweas, A. F., Osman, H.-E. H., Naguib, I. A., Abourehab, M. A. S. & Abdel-Moneim, A. S. (2022). Virtual Screening of Repurposed Drugs as Potential Spike Protein Inhibitors of Different SARS-CoV-2 Variants: Molecular Docking Study. *Current Issues in Molecular Biology*, 44 (7), 3018–3029. https://doi.org/10.3390/cimb44070208
13. Fan, Y., Zhao, K., Shi, Z. L., & Zhou, P. (2019). Bat coronaviruses in China. In *Viruses*,11 (3). MDPI AG. https://doi.org/10.3390/v11030210
14. Gholap, S. S. (2016). Pyrrole: An emerging scaffold for construction of valuable therapeutic agents. *European Journal of Medicinal Chemistry*, 110, 13–31. https://doi.org/10.1016/j.ejmech.2015.12.017
15. Ibba, R., Piras, S., Corona, P., Riu, F., Loddo, R., Delogu, I., Collu, G., Sanna, G., Caria, P., Dettori, T. & Carta, A. (2021). Synthesis, Antitumor and Antiviral In Vitro Activities of New Benzotriazole-Dicarboxamide Derivatives. *Frontiers in Chemistry*, 9. https://doi.org/10.3389/fchem.2021.660424
16. Jayaram, B., Singh, T., Mukherjee, G., Mathur, A., Shekhar, S. & Shekhar, V. (2012). Sanjeevini: a freely accessible web-server for target directed lead molecule discovery. *BMC Bioinformatics*, 13 (S17), S7. https://doi.org/10.1186/1471-2105-13-S17-S7
17. Ji, D., Xu, M., Udenigwe, C. C. & Agyei, D. (2020). Physicochemical characterisation, molecular docking, and drug-likeness evaluation of hypotensive peptides encrypted in flaxseed proteome. *Current Research in Food Science*, 3, 41–50. https://doi.org/10.1016/j.crfs.2020.03.001
18. Khramtsova, E. E., Dmitriev, M. V., Bormotov, N. I., Serova, O. A., Shishkina, L. N., & Maslivets, A. N. (2021). Alkaloid-like annulated pyrano[4,3-b]pyrroles: antiviral activity and hydrolysis. *Chemistry of Heterocyclic Compounds*, 57 (4), 483–489. https://doi.org/10.1007/s10593-021-02928-0
19. Lin, J. H., & Yamazaki, M. (2003). Role of P-glycoprotein in pharmacokinetics: clinical implications. *Clinical Pharmacokinetics*, 42 (1), 59–98. https://doi.org/10.2165/00003088-200342010-00003
20. Lipinski, C. A. (2004). Lead- and drug-like compounds: the rule-of-five revolution. *Drug Discovery Today. Technologies*, 1 (4), 337–341. https://doi.org/10.1016/j.ddtec.2004.11.007
21. Lu, R., Zhao, X., Li, J., Niu, P., Yang, B., Wu, H., Wang, W., Song, H., Huang, B., Zhu, N., Bi, Y., Ma, X., Zhan, F., Wang, L., Hu, T., Zhou, H., Hu, Z., Zhou, W., Zhao, L., … Tan, W. (2020). Genomic characterisation and epidemiology of 2019 novel coronavirus: implications for virus origins and receptor binding. *The Lancet*, 395 (10224), 565–574. https://doi.org/10.1016/S0140-6736(20)30251-8
22. Mostafa, A., Kandeil, A., A M M Elshaier, Y., Kutkat, O., Moatasim, Y., Rashad, A. A., Shehata, M., Gomaa, M. R., Mahrous, N., Mahmoud, S. H., GabAllah, M., Abbas, H., Taweel, A. El, Kayed, A. E., Kamel, M. N., Sayes, M. El, Mahmoud, D. B., El-Shesheny, R., Kayali, G. & Ali, M. A. (2020). FDA-Approved Drugs with Potent In Vitro Antiviral Activity against Severe Acute Respiratory Syndrome Coronavirus 2. *Pharmaceuticals (Basel, Switzerland)*, 13 (12). https://doi.org/10.3390/ph13120443
23. Naqvi, A. A. T., Fatima, K., Mohammad, T., Fatima, U., Singh, I. K., Singh, A., Atif, S. M., Hariprasad, G., Hasan, G. M. & Hassan, M. I. (2020). Insights into SARS-CoV-2 genome, structure, evolution, pathogenesis and therapies: Structural genomics approach. In *Biochimica et Biophysica Acta - Molecular Basis of Disease*, 1866 (10). Elsevier B.V. https://doi.org/10.1016/j.bbadis.2020.165878
24. Neuman, B. W., Adair, B. D., Yoshioka, C., Quispe, J. D., Orca, G., Kuhn, P., Milligan, R. A., Yeager, M. & Buchmeier, M. J. (2006). Supramolecular Architecture of Severe Acute Respiratory Syndrome Coronavirus Revealed by Electron Cryomicroscopy. *Journal of Virology*, 80 (16),

7918–7928. https://doi.org/10.1128/jvi.00645-06
25. Newman, J. A., Douangamath, A., Yadzani, S., Yosaatmadja, Y., Aimon, A., Brandão-Neto, J., Dunnett, L., Gorrie-stone, T., Skyner, R., Fearon, D., Schapira, M., von Delft, F. & Gileadi, O. (2021). Structure, mechanism and crystallographic fragment screening of the SARS-CoV -2 NSP13 helicase. *Nature Communications*, 12 (1). https://doi.org/10.1038/s41467-021-25166-6
26. O'Boyle, N. M., Banck, M., James, C. A., Morley, C., Vandermeersch, T., & Hutchison, G. R. (2011). Open Babel: An open chemical toolbox. *Journal of Cheminformatics*, 3, 33. https://doi.org/10.1186/1758-2946-3-33
27. Pal, M., Berhanu, G., Desalegn, C. & Kandi, V. (2020). Severe Acute Respiratory Syndrome Coronavirus-2 (SARS-CoV-2): An Update. *Cureus*, 12 (3), e7423. https://doi.org/10.7759/cureus.7423
28. Perez-Lemus, G. R., Menéndez, C. A., Alvarado, W., Byléhn, F. & de Pablo, J. J. (2022). Toward wide-spectrum antivirals against coronaviruses: Molecular characterization of SARS-CoV-2 NSP13 helicase inhibitors. *Science Advances*, 8 (1), eabj4526. https://doi.org/10.1126/sciadv.abj4526
29. Rastogi, M., Pandey, N., Shukla, A. & Singh, S. K. (2020). SARS coronavirus 2: from genome to infectome. In *Respiratory Research,* 21 (1). BioMed Central Ltd. https://doi.org/10.1186/s12931-020-01581-z
30. Smith, E. C., Blanc, H., Vignuzzi, M. & Denison, M. R. (2013). Coronaviruses Lacking Exoribonuclease Activity Are Susceptible to Lethal Mutagenesis: Evidence for Proofreading and Potential Therapeutics. *PLoS Pathogens*, 9 (8). https://doi.org/10.1371/journal.ppat.1003565
31. Subissi, L., Imbert, I., Ferron, F., Collet, A., Coutard, B., Decroly, E. & Canard, B. (2014). SARS-CoV ORF1b-encoded nonstructural proteins 12-16: Replicative enzymes as antiviral targets. In *Antiviral Research*, 101 (1), 122–130. https://doi.org/10.1016/j.antiviral.2013.11.006
32. Tanner, J. A., Watt, R. M., Chai, Y. B., Lu, L. Y., Lin, M. C., Peiris, J. S. M., Poon, L. L. M., Kung, H. F. & Huang, J. D. (2003). The severe acute respiratory syndrome (SARS) coronavirus NTPasefhelicase belongs to a distinct class of 5′ to 3′ viral helicases. *Journal of Biological Chemistry*, 278 (41), 39578–39582. https://doi.org/10.1074/jbc.C300328200
33. Tanner, J. A., Zheng, B.-J., Zhou, J., Watt, R. M., Jiang, J.-Q., Wong, K.-L., Lin, Y.-P., Lu, L.-Y., He, M.-L., Kung, H.-F., Kesel, A. J. & Huang, J.-D. (2005). The adamantane-derived bananins are potent inhibitors of the helicase activities and replication of SARS coronavirus. *Chemistry & Biology*, 12 (3), 303–311. https://doi.org/10.1016/j.chembiol.2005.01.006
34. Walker, J. E., Saraste, M., Runswick, M. J. & Gay, N. J. (1982). Distantly related sequences in the alpha- and beta-subunits of ATP synthase, myosin, kinases and other ATP-requiring enzymes and a common nucleotide binding fold. *The EMBO Journal*, 1 (8), 945–951. https://doi.org/10.1002/j.1460-2075.1982.tb01276.x
35. Wang, Z., Huang, J.-D., Wong, K.-L., Wang, P.-G., Zhang, H.-J., Tanner, J. A., Spiga, O., Bernini, A., Zheng, B. J. & Niccolai, N. (2011). On the mechanisms of bananin activity against severe acute respiratory syndrome coronavirus. *The FEBS Journal*, 278 (2), 383–389. https://doi.org/10.1111/j.1742-4658.2010.07961.x